PROCEEDINGS OF SCIENCE

# The ultimate CMS ECAL calibration and performance for the legacy reprocessing of LHC Run 2 data

**Raffaella Tramontano, on behalf of the CMS Collaboration.**[a,*]

[a] *Sapienza, University of Rome and Istituto Nazionale di Fisica Nucleare, Sezione di Roma, Italy*

*E-mail:* raffaella.tramontano@cern.ch

Many physics analyses using the Compact Muon Solenoid (CMS) detector at the LHC require accurate, high resolution electron and photon energy measurements. Excellent energy resolution is crucial for studies of Higgs boson decays with electromagnetic particles in the final state, as well as searches for very high mass resonances decaying to energetic photons or electrons. The CMS electromagnetic calorimeter (ECAL) is a fundamental component of these analyses, and its energy resolution is crucial for the Higgs boson mass measurement. It also provides a measurement of the electromagnetic component of jets, and contributes to the measurement of calorimeter energy sums, both of which are important for a wide range of CMS physics analyses.

Recently the energy response of the calorimeter has been precisely calibrated exploiting the full Run 2 (2015-18) dataset, and has been used for legacy reprocessing of the data. A dedicated calibration of each detector channel has been performed with physics events exploiting electrons from W and Z boson decays, photons from $\pi^0/\eta^0$ decays, and from the azimuthally symmetric energy distribution of minimum bias events. This talk presents the calibration strategies that have been implemented and the improved ECAL performance that has been achieved with the ultimate calibration of Run II data, in terms of energy scale stability and energy resolution. The calibration plans currently being developed to achieve and maintain optimum performance during LHC Run 3 (2022-25) will also be discussed.

*41st International Conference on High Energy physics - ICHEP2022*
*6-13 July, 2022*
*Bologna, Italy*

*Speaker





PoS(ICHEP2022)643

## 1. Introduction

The Compact Muon Solenoid (CMS) [1] experiment at the CERN Large Hadron Collider is equipped with a scintillating crystal electromagnetic calorimeter (ECAL). ECAL is a homogeneus, hermetic, high granularity scintillating lead tungstate ($PbWO_4$) crystal calorimeter for high precision measurements of the energy of photons and electrons. It is composed of roughly 75000 crystals, divided into a barrel section (EB), covering the pseudorapidity region $|\eta| < 1.479$, and an endcap section (EE) consisting of two disks, covering the $1.479 < |\eta| < 3.0$ region. A preshower system of lead and silicon strips is installed in front of the endcap ECAL for $\pi^0$ rejection. ECAL crystals convert energy into light, and the scintillation light is detected by silicon avalanche photodiodes (APDs) in the barrel region and vacuum phototriodes (VPTs) in the endcap region.

ECAL energy resolution performance is crucial for searches and analyses involving energetic photons and electrons, such as the Higgs boson decay in two photons. Continuos monitoring of environmental effects and radiation induced light output changes is required to ensure and maintain optimal energy resolution performances in crystal calorimeters. The reconstruction and calibration strategy put in place throughout ECAL operational years to monitor and improve the energy resolution performances is presented in this work. The high instantaneous luminosities (up to $2 \cdot 10^{34} cm^{-2} s^{-1}$) and increased number of overlapping interactions per bunch crossing ( pile up, up to 40) delivered in LHC Run 2 have provided challenging operational conditions for the detector. A particular focus will be therefore put on the motivation and outcomes of the recent ECAL calibration campaign for CMS Run 2 Legacy data reprocessing.

## 2. ECAL energy reconstruction and calibration

Photons and electrons energy measurement in ECAL are performed by detecting electromagnetic showers developing within lead tungstate crystals. The energy deposited by an electromagnetic shower in ECAL is reconstructed according to (1)

$$E_{e,\gamma} = \sum_i [A_i(t) \cdot L_i(t) \cdot C_i(t)] \cdot G(\eta) \cdot F_{e,\gamma} + E_{preshower} \quad (1)$$

The sum runs over a set of i crystals involved in the electromagnetic showers (a crystal "SuperCluster") and $A_i(t)$ is the signal amplitude, extracted by the APD ADC. The amplitude measurement is corrected to account for multiple environmental effects. Crystal to crystal corrections, $L_i(t)$ and $C_i$(t) in (1), are applied to respectively correct for radiation driven loss of crystal transparency , and to ensure a homogeneous energy measurement output through the detector.
The corrected per crystal amplitudes are then summed in an electromagnetic deposit energy estimate. The $G(\eta)$ term is used to convert ADC counts in energy estimates, and is derived by calibration of ECAL energy measurements over the $\pi^0$ and Z Standard Model candles. Finally, refinement corrections depending on the reconstructed type of particle, $F_{e,\gamma}$ are applied to account for imperfect clustering procedure, geometric and material effects. he preshower energy is finally added to the estimate.

In the following subsections, a description of the strategies put in place for each calibration step is presented.

### 2.1 Signal amplitude reconstruction

ECAL single crystal energy measurement is performed by estracting the APD signal pulse amplitude. The signal shape and pedestal information are fundamental for the amplitude extraction procedure: they are continuously monitored and corrected to ensure proper modeling.

Crystals light transmission decreases with radiation damage, leading to changes in the shape of the collected pulse. During Run 2, pulse shapes for signal extractions were recomputed every 3-4 $fb^{-1}$ to accomodate for shape evolution with increasing radiation.

Amplitude pedestals, on the other hand, depend mostly on APDs behavior: a ~40 MeV/year increase in pedestal absolute value has been observed in average throughout ECAL operational years. Monitoring of the pedestals value and spread has been performed in Run 2 by collecting pedestal runs every 40 minutes, using the same laser system presented in Section 2.2 for radiation damage monitoring.

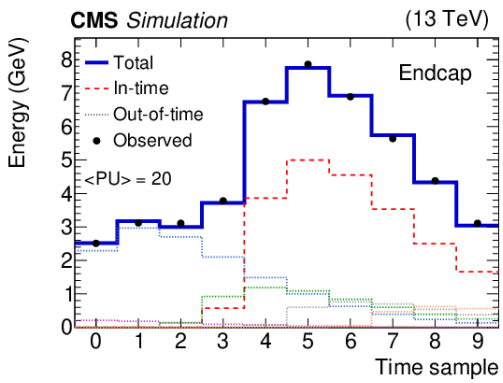


**(a)** Multifit fitting procedure example. An in time pulse in red is fitted together with a late pulse (grey) and several early pulses

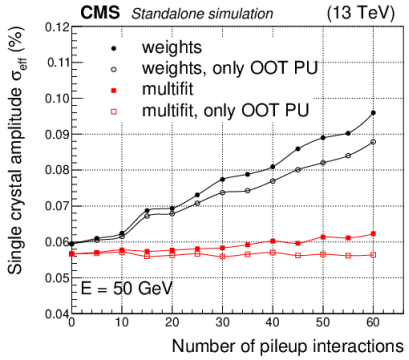


**(b)** Comparison of the multifit (red) and weights (black) algorithms single crystal amplitude $\sigma_{eff}$ as a function of the number of overlapping interactions (pile up).

**Figure 1**

The ECAL amplitude reconstruction changed from Run1 to Run 2, adapting to the higher pile up conditions of LHC collisions. The Multifit [2] algorithm specifically treats overlapping signal amplitudes in the same crystal by fitting the pulse shape with a single in time pulse and up to 9 out of time pulses. An example of the fitted signal pulse and its components is presented in Figure 1a. The time offset of the 9 out of time pulses are left floating, together with the signal amplitudes, while the pulse shape is fixed.

The performance in single crystal effective signal width, $\sigma_{eff}$, of the Multifit algorithm with respect to Run 1 weights algorithm for APD signal extraction is presented in Figure 1b, as a function of the number of simultaneous interactions. The multifit performance results stable with increasing pile up, whereas the weights algorithm shows worsening performaces in $\sigma_{eff}$ with increasing simultaneous interctions.

### 2.2 Crystal ageing corrections

LHC proton-proton collisions struck the detector with extreme radiation rates. Crystal light transmission and, consequently, light output, are heavily influenced by the radiation damage. Transparency loss impacts pulse shapes on very short times scales and it is heavier at high $\eta$, where crystals

are subjected to higher radiation rates. A moderate transparency recovery can be obtained in lead tungstate crystals by annealing at room temperature.

ECAL is equipped with a dedicated laser + LED monitoring system [3] which is used to asses the transparency loss within each crystal. A crystal-by-crystal laser scan is performed every 40 minutes during data-taking, to derive time dependent crystal transparency corrections. The relation between crystal response to laser light and to an electromagnetic shower signal can be modeled as :

$$\frac{S}{S_0} = \left(\frac{L}{L_0}\right)^{\alpha} \tag{2}$$

where $L_0$ and $S_0$ are reference responses to laser light and electromagnetic shower measured at the beginning of each data taking and the exponent $\alpha$ is measured to be ~1.5 in the barrel and between 0.6 and 1.1 in the endcaps. The normalized $\pi_0$ mass of two photon deposits in ECAL is reported in Figure 2,

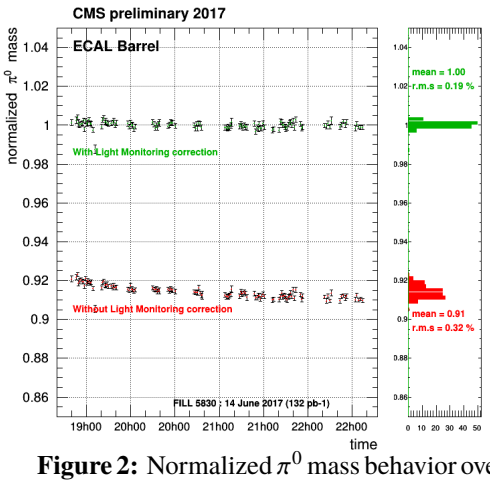


**Figure 2:** Normalized $\pi^0$ mass behavior over a few hours data-taking period with (green) and without (red) laser corrections applied.

with (green) and without (red) laser corrections, as a function of time. The impact of laser corrections is impressive, as it allows for full recovery of the correct measurements for the photon energies and, consequently, $\pi^0$ mass. The uncorrected $\pi^0$ mass absolute value and resolution worsens over a few hours time range, thus deeming a fine-grained in time correction necessary for optimal energy measurement recovery.

Residual response losses were observed on yearly time scales through Run 2, due to radiation damage on laser reference diodes and transmission fibers. The effect is corrected exploiting the E/p ratio of the electromagnetic energy measurement over the particle transverse momentum as measured in CMS tracker, for electrons coming from W and Z bosons decays.

### 2.3 Crystal Inter-calibrations

Inter-calibration coefficients are used to correct the single crystal output to ensure an homogeneus response behavior over the detector. CMS currently exploits three independent methods for inter-calibration coefficient derivation: $\pi^0 \to \gamma\gamma$ and $Z \to e^+e^-$ based calibrations and E/p ratios with p transverse momentum as measured from the tracker . The inter-calibration outputs from those techniques are then combined in a single, per crystal, inter-calibration correction.

$\pi^0 \to \gamma\gamma$ *inter-calibrations:* a $\pi^0$ invariant mass spectrum is built considering all the $\gamma\gamma$ candidates for which one of the photons has deposited a fraction of its energy in a crystal. The mass shift between the measured peak position and the PDG [4] mass value for $\pi^0$ is used to derive an energy correction to be applied to the crystal. The calibration algorithm proceeds iteratively correcting each crystal output by the observed mass peak shift, equalizing the channel response in rings of fixed azimuth.

*E/p calibrations* exploit the independent transverse momentum measurement for electrons in the CMS tracker. A set of high energy electrons from $W^{\pm}$ and Z decays is selected through

a combination of kinematic cuts, identification and isolation criteria. The calibration algorithm iteratively assigns a coefficient to each crystal, such that the average E/p ratio for such high purity electron dataset is constrained to 1.

$Z \to e^+e^-$ *inter-calibrations*: the method has been introduced in Run 2 thanks to the high per year integrated available luminosity, which allowed to performed per crystal calibrations on a high energy, smaller cross section resonance. The crystal by crystal calibration consists in the maximization of a likelihood comparing the reconstructed mass distribution with that predicted by Monte Carlo simulation.

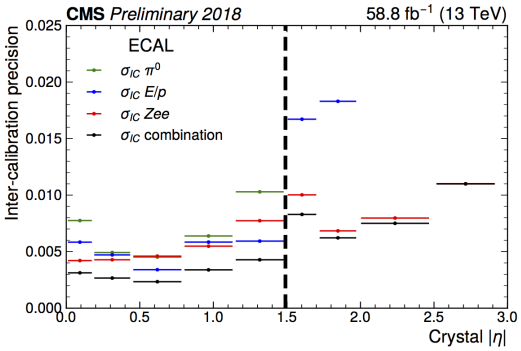


**Figure 3:** Intercalibration precision as a function of pseudorapidity with the 2018 dataset. The red, blue and green points represent performaces for three different inter-calibration methods, while their combination is reported in the black points .

The three calibration methods are combined and their performances is assessed in term of the calibration method precision. The precision of each method and of their combination is reported in Figure 3. The overall inter-calibration precision is smaller than 1% and decreases to less than 0.5% in the barrel region. The novel $Z \to e^+e^-$ calibration method drives the inter-calibration precision in the high $\eta$ region. The $2.5 < |\eta| < 3.0$ region in particular is out of tracker coverage, hence the ability to calibrate ECAL energy response becomes crucial for very forward jets energy reconstruction.

### 2.4 Energy measurements refinements

A semiparametric Boosted Decision Tree regression is put in place to recover possible performance losses due to electroamagnetic shower leakages, dead channels and material and geometric effects. The regression algorithm exploits variables related to the electromagnetic shower shape and dimension, the supercluster isolation and, for electrons, bremsstrahlung energy loss and the angular coordinates of the track matched to the SuperCluster. A detailed description of ECAL regression algorithm is reported in [5].

## 3. Run 2: legacy reprocessing and performance

A calibration exploiting the full Run2 dataset has been performed for the CMS Legacy reprocessing. The comparison between the pre-legacy and legacy ECAL performance is presented in Figure 4a. A set of refined corrections, fine grained in both time and data taking conditions, has lead to an overall improvement in the resolution performance of ~40 %.

The simulated contributions of the reconstruction and calibration steps to ECAL energy resolution are reported in Figure 4b, for 2018 data taking conditions. The intercalibration impact is negligible, while noise and pile up yield significant and comparable contributions to the total resolution. Unaccounted effects are also significant: they can be described through a gaussian smearing applied to simulation to match the performance in data and result stable over time.

## 4. Conclusions

ECAL reconstruction and calibration are crucial to deliver and maintain the best energy resolution performance. Multiple novel strategies in both signal amplitude fitting and calibration

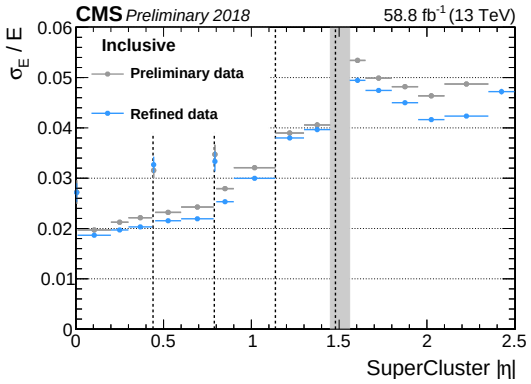


**(a)** ECAL resolution performance as a function of pseudorapidity for 2018 data. for standard early data calibrated data in grey, Legacy calibrated dataset in light blue.

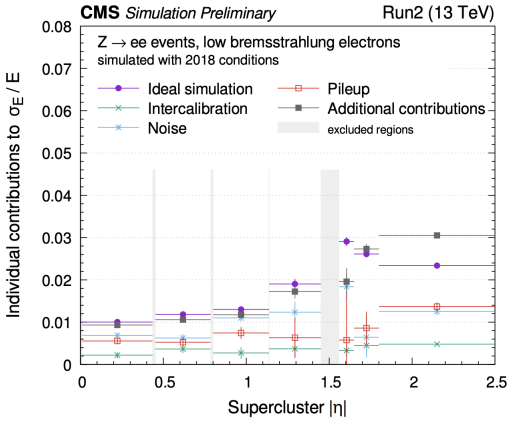


**(b)** Simulated resolution contributions breakdown as a function of pseudorapidity.

**Figure 4**

techinques have been implemented, tested and optimized throughout Run2. ECAL energy resolution performance through LHC operational years is reported in Figure 5. Run 2 performances, after the Legacy reprocessing, are comparable to ECAL energy resolutions measured for Run 1. This configures as an exceptional result, as both pile up increase through Run 2 and increasing radiation damage have dramatically changed inbetween the two LHC Runs.

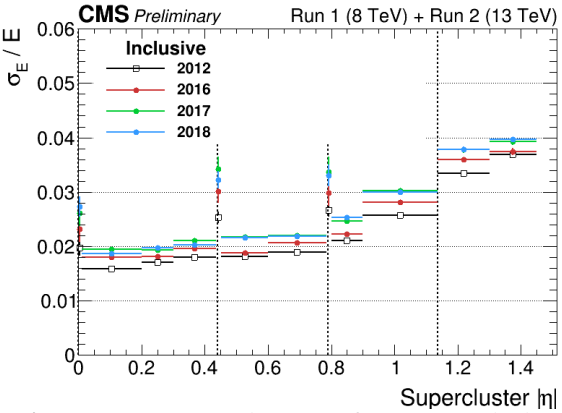


**Figure 5:** ECAL resolution performance in the barrel region through Run 1 and Run 2 operational years.

The Legacy reprocessing has proven the power of fine grained calibrations in terms of time and detector geometry. As Run 3 and the High Luminosity LHC program are approaching, ECAL calibration main goals are rooting towards the development of authomatic workflow to deliver on-line corrections during data taking. As pile up will continue to increase, the exploitation of ECAL timing measurement will become crucial to allow for discrimination of overlapping signals. Developments in this direction will be boosted by the novel barrel front-end electronics that will be installed for CMS HL-LHC upgrade.

## References

[1] CMS Collaboration, 2008 *The CMS experiment at the CERN LHC*, JINST 3 S08004

[2] CMS Collaboration, 2020, *Reconstruction of signal amplitudes in the CMS electromagnetic calorimeter in the presence of overlapping proton-proton interactions*, JINST 15 (2020) 10, P10002

[3] ] M. Anfreville et al., 2008 *Laser monitoring system for the CMS lead tungstate crystal calorimeter*, Nuclear Instruments and Methods in Physics Research, A 594 2:292-320

[4] Particle Data Group, 2016 *Review of Particle Physics*, 2016-2017 Chin. Phys. C 10 40:100001

[5] CMS Collaboration, 2020, *Electron and photon reconstruction and identification with the CMS experiment at the CERN LHC*,JINST 16, 05 (2021) pp.P05014